# The effect of head-forward posture on risk of lower neck dislocation during head-first impacts: a preliminary computational and dynamic experimental investigation

Mario Mongiardini, Aaron Stevenson, Claire F. Jones, Ryan D. Quarrington

## I. INTRODUCTION

Subaxial cervical facet dislocation (CFD) is a severe neck injury that most often results from head-first impacts (HFI), wherein head motion is arrested and the following torso compresses the neck [1]. Despite the established causal link between HFI and CFD, and decades of laboratory research, replicating CFD in experimental and computational HFIs has proven challenging. The lack of repeatable dynamic models of subaxial CFD highlights gaps in understanding of its underlying mechanisms, thereby hindering the advancement of effective injury prevention devices and strategies. Prior investigations have produced subaxial CFD by applying quasi-static axial compression to C0-T1 specimens and permitting anterior C0 translation while maintaining a horizontal Frankfort plane (FP) [2-3]. However, these head-end boundary conditions likely diverge from the dynamics of a real-life HFI event, where inertia resists head motion during the neck injury event (~20 ms post-HFI) [4]. Nonetheless, the eccentric head-forward posture (HFP) created in these quasi-static experiments might elevate the risk of CFD during an actual HFI. The aims of this ongoing study are to: (A) use computer simulations to investigate the effect of pre-HFI head eccentricity and FP angle on head-neck kinematics, kinetics, and CFD risk; (B) establish an experimental HFI *ex-vivo* CFD model; and, (C) verify the HFI computer simulations and inform improvements.

## II. METHODS

***Aim A – Computational modelling:*** HFI has been simulated using a modified version of the Global Human Body Models Consortium 50th percentile male detailed head-neck model (GHBMC M50-HN, Version 6.0). To match the experiments (Fig 1), the neck flesh, all musculature, tendons, hyoid bone and mandible, and all attachments, were removed from the GHBMC M50-HN. The model was rotated so T1 was 25° to horizontal [3-4], and the inferior portion of T1 was rigidly connected to geometrical representations of the potting mold, 6-axis load cell, and overhead drop carriage (16 kg effective torso mass [4]). To simulate the drop rail, this carriage assembly was constrained to vertical translation only. The coefficient of friction between the head and the aluminium impact plate used in the experiments was measured and assigned to the rigid impact surface ($\mu = 0.52$). To explore pre-HFI combinations of head eccentricity (C0-T1 horizontal distance; 0 to 50 mm, 5 mm increments) and FP angle (30° extension to 30° flexion, 5° increments), each simulation comprised initial model reposturing followed by a stress-retaining restart simulating the HFI (2 m/s velocity). Impact surface, drop carriage, and intervertebral loads, and kinematics, were extracted.

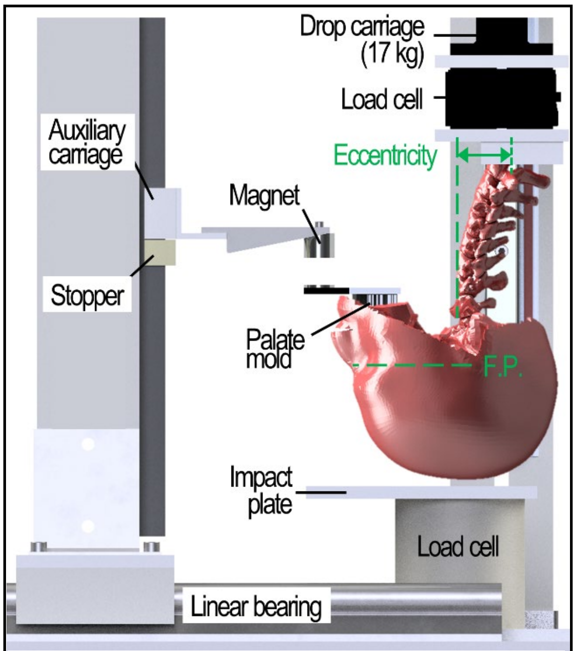


**Fig 1** Schematic of the head-first impact experiments.

***Aim B – Drop tower experiments***: To verify the simulations and establish testing protocols, two fresh-frozen human cadaver osteoligamentous head-necks (1×Ceph-T1, 1×Ceph-C7) have undergone inverted HFI pilot experiments using a drop tower (HREC approval H-2023-098); the FP was horizontal and head eccentricity were 30 and 20 mm, respectively. The drop-height was 240 mm for a 2 m/s head-impact velocity (35 Joules). Head-neck posture was maintained during the drop via an auxiliary parallel drop rail; the auxiliary carriage interfaced with the head via a specimen-specific, 3D-printed hard palate mount (Fig 1). The geometry of the mount ensured a horizontal FP and the position of the auxiliary rail was adjusted, via a lockable linear bearing, to achieve the desired eccentricity. Head constraints were removed immediately prior to impact via external-trigger release of an electromagnet that connected the palate mount and the auxiliary carriage. Impact surface and caudal loads were measured by 6-axis load cells and carriage position was measured with a linear encoder (both 50 kHz). Kinematics were measured by tracking three-marker clusters embedded at each spinal level, and in the cephalus, using stereo-calibrated high-speed cameras (Phantom VEO1010; 10 kHz). Injuries were identified via post-test

R. D. Quarrington is a Grant Funded Research Fellow in the Adelaide Medical School at The University of Adelaide, Australia (+61418560917, ryan.quarrington@adelaide.edu.au). M. Mongiardini is a Grant Funded Research Fellow with the Centre for Automotive and Safety Research at The University of Adelaide. A. Stevenson is the Head of the Spinal Surgery Unit at the Royal Adelaide Hospital. C. F. Jones is an Associate Professor in the School of Electrical and Mechanical Engineering at The University of Adelaide.

inspection and CT scan. Qualitative kinematic analyses of the simulation and experimental data were performed; loads at key timepoints were extracted.

## III. INITIAL FINDINGS

To date, HFI simulations have been completed for three head-neck postures with horizontal FP: 0 mm (neutral [$Ecc_N$]), 30 mm [$Ecc_S$], and 50 mm [$Ecc_L$] eccentricity. In all simulations, the torso started compressing the neck ~1 ms after head impact, forcing the upper head-neck into extension and C7/T1 into flexion ("buckled" neck pose [1]) without concomitant head translation (Fig 2C). Additional torso compression caused failure of C7/T1 supra- and interspinous ligaments. Subsequent head extension rotation and forward motion caused C7/T1 anterior shear translation (Fig 2E). Peak T1 compression forces were similar for all simulations (2.25-2.32 kN) but peak C7/T1 anterior shear force (the primary contributor to CFD [1]) was largest for $Ecc_S$ (650.7 N, 315.0% and 29.6% ↑ than $Ecc_N$ and $Ecc_L$, respectively). Therefore, the $Ecc_S$ pre-HFI posture was investigated experimentally in two pilot tests. To account for the absence of T1, 20 mm eccentricity was applied in Test #2. Bilateral CFD was produced at the embedded caudal level in both (+C7 fracture in Test #2), with concomitant C3/C4 extension injuries. Kinematics and kinetics preceding CFD closely followed the $Ecc_S$ simulation (Fig 2), but existing limitations of the failure criteria for the facet capsule and intervertebral discs (IVD) prevented CFD in the simulation.

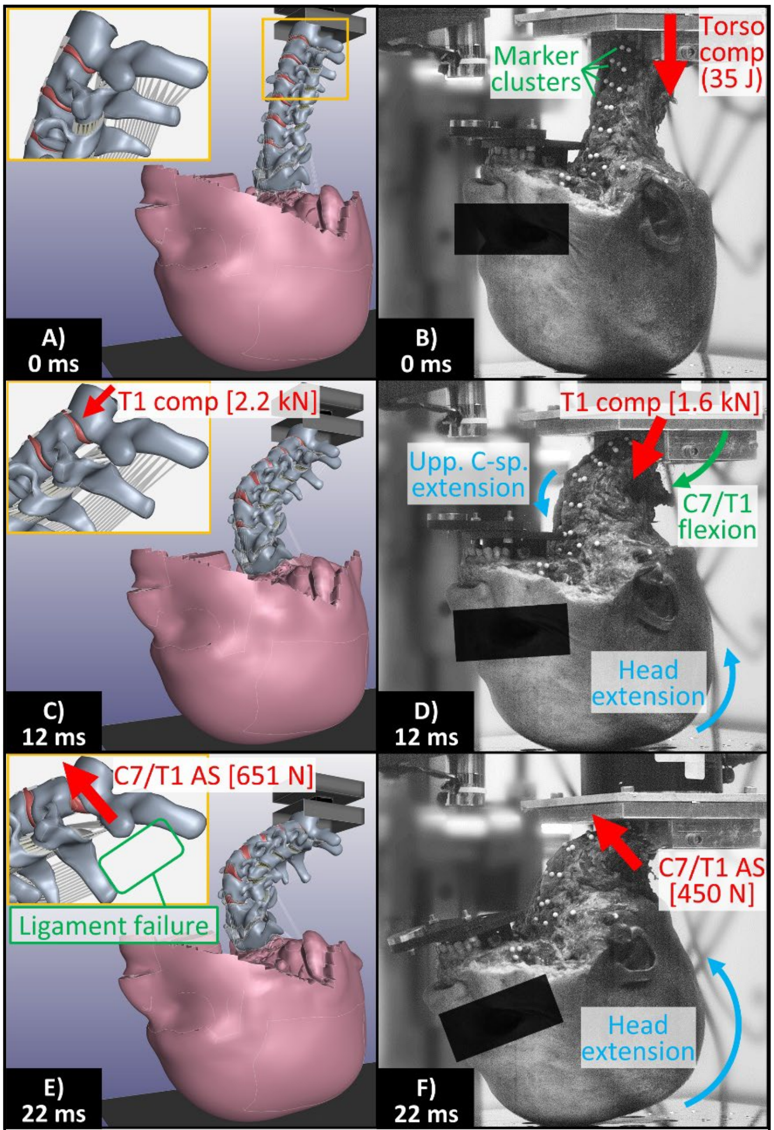


**Fig 2** Computer [left] and experimental HFI [Test #1, 30 mm eccentricity]. A-B) Onset of neck loading from torso. C-D) Upper extension, C7/T1 hyperflexion. E-F) C7/T1 anterior shear [AS] causing experimental CFD.

## IV. DISCUSSION

Detailed data analysis is ongoing, but these preliminary results indicate that the risk of lower neck dislocation is highly sensitive to pre-HFI head eccentricity, when the FP is horizontal. This result supports the hypothesis of Pintar *et al.* [5] that HFI-related CFD (described as "major hyperflexion" injury) is associated with a C0-T1 eccentricity of 31 mm, while larger eccentricities (>70 mm) reduce risk of severe neck injury; however, a horizontal FP was not maintained in those experiments. Our pilot data also suggests that this HFP can produce neck trauma at lower impact velocities (2 m/s) than previously reported [4]. Comparison of the simulations and experiments revealed some limitations of the GHBMC M50-HN during HFI. Bone element erosion was disabled after unrealistic C0 fractures were predicted for low-energy impacts [4], while failure criteria limitations for the capsular ligament and IVD prevented CFD from occurring despite sufficient intervertebral shear force [6]. Unrealistic post-HFI head bouncing was also observed, likely due to the scalp material definition. Despite these limitations, the GHBMC M50-HN appropriately simulated the pre-CFD head-neck response to HFI and will be used to identify the HFP for our *ex-vivo* HFI model of CFD.

## V. ACKNOWLEDGEMENTS

L Sweet for early model developments. D Cronin for guidance. The Adelaide Medical School Body Donor Program. Lifetime Support Authority for project funding (R2230).

## VI. REFERENCES

[1] Nightingale, *et al.*, *Clin Biomech*, 2019. [2] Bauze, *et al.*, *J Bone Joint Surg*, 1978. [3] Nightingale, *et al.*, *Stapp J*, 1991. [4] Nightingale, *et al.*, *J Biomech*, 1996. [5] Pintar, *et al., J Neurosurg: Spine,* 2002. [6] Quarrington, *et al., JBME*, 2021.